# Aharonov-Bohm oscillations in a hydrogen atom in a radiation field through electron self-interference

Maciej Kalinski
*Rochester Theory Center for Optical Science and Engineering and Department of Physics and Astronomy, University of Rochester, Rochester, New York 14627*
(Received 3 March 1997)

We study the influence of a weak magnetic field on time evolution of a quantum state that is a coherent superposition of two counter-rotating Trojan wave packets in a linearly polarized electromagnetic field. We demonstrate that both the interference pattern of the electron probability density and differential cross section for half-cycle pulse ionization exhibit periodic modulation as a function of magnetic flux cutting the plane of packet motion. The shift is proportional to the magnetic flux in a way characteristic for the Aharonov-Bohm effect. [S1050-2947(98)06202-7]

PACS number(s): 32.80.Rm, 42.50.Hz, 03.65.Bz, 03.75.Dg

An experiment has recently been performed showing that it is possible to generate an electron with radially dual spatial nature, namely, localized at two places at the same time [1]. This new experimental method makes it possible to observe interference fringes between two ''parts'' of a single electron analogous to those observed in a macroscopic Young experiment. This state is a coherent superposition of two radially confined electron wave packets that later spread and revive as a result of the nonlinearity of the Coulomb spectrum [2,3].

The influence of magnetic flux on electron interference has been a subject of both experimental and theoretical studies for many years [4]. These have been studies of the Aharonov-Bohm (AB) effect [5,6] as well as of a direct influence of the magnetic flux on the physical properties of the quantum system when the magnetic field itself is also present [4,7]. Both macroscopic and mesoscopic systems have been the subject of those studies [8].

The common characteristic feature of this influence is that the physical quantities of the system depend periodically on the magnetic flux that passes through the system with a period related to the quantum of the magnetic flux $h/2e$.

In the following we study numerically quantum states of hydrogen in linearly polarized electromagnetic and magnetic fields. We construct these states as coherent superpositions of well localized states in a circularly polarized field called Trojan wave packets [9–11]. They can be used in an experiment analogous to the one reported in [1] but with an addition of a weak magnetic field. We present the results of numerical simulations that show that the presence of the magnetic flux leads to Aharonov-Bohm oscillations of the electron probability density as well as magnetic field oscillatory dependence of differential cross section for ultrashort half-cycle pulse ionization.

It has been shown theoretically [9,10] that it is possible to generate and control the time evolution of a quantum state of hydrogen, whose probability density represents a well localized wave packet in three spatial dimensions moving around a classical circular orbit [12] without dispersion. In the laboratory frame this state is a time-dependent solution of the Schrödinger equation with the Hamiltonian

$$H_t=\mathbf{p}^2/2-1/|\mathbf{r}|+\mathbf{r}\cdot\vec{E}_{\pm}(t), \tag{1}$$

where

$$\vec{E}_{\pm}(t)=\mathcal{E}\,[\hat{x}\cos\omega t\pm\hat{y}\sin\omega t], \tag{2}$$

and it can be approximated by a Gaussian wave function with a center moving around a circular trajectory [10]

$$\Phi_{\pm}(\mathbf{r},t)=Ne^{\pm i(n_0-1)\phi}e^{-(\omega/2)(r-r_0)^2}\times e^{-(\omega/2)r_0^2\theta^2}e^{-\beta(\omega/2)r_0^2(\phi\mp\omega t)^2}. \tag{3}$$

The angular confinement of the packet can be controlled by the strength of the circularly polarized field since $\beta=(\mathcal{E}/3)^{1/2}\omega^{-2/3}$. Similar electron confinement can be obtained using a strong magnetic field in addition to the circularly polarized field [13].

We first consider the leading effect of a weak magnetic field on the Trojan packet evolution in a circularly polarized electromagnetic field. The quantum mechanical Hamiltonian of a hydrogen atom in both circularly polarized electromagnetic and static magnetic fields can be written in a frame rotating with a field as

$$H=\mathbf{p}^2/2-1/r+\mathcal{E}x-(\omega\mp\omega_c/2)L_z+\tfrac{1}{8}\omega_c^2(r^2-z^2), \tag{4}$$

where $\omega_c$ is the cyclotronic frequency of the magnetic field $B$ ($\omega_c=B$ in atomic units). Considering only weak magnetic fields ($\omega_c\ll\omega$) we drop first the diamagnetic term in Hamiltonian (4) proportional to $\omega_c^2$. The remaining paramagnetic term has the same structure as the term that appears because of the rotation of the coordinate system and we can also obtain an effective pendular Hamiltonian in every subspace of hydrogenic states with a fixed deviation from circularity [9,14]. The resulting Hamiltonian is now

$$\mathcal{H}=\frac{3}{2}\frac{1}{r_0^2}\frac{\partial^2}{\partial\phi^2}\pm i\frac{\omega_c}{2}\frac{\partial}{\partial\phi}+\mathcal{E}r_0\cos\phi, \tag{5}$$

with $r_0=n_0^2$, $\omega=1/n_0^3$ and it differs from the Hamiltonian discussed in [10] only by the linear term $\mp\frac{1}{2}\omega_cL_z$. The eigenvalues $E^j$ of the Hamiltonian (4) (with diamagnetic term neglected) can be written in terms of the eigenvalues of the Hamiltonian (5) as

 

$$E^j_{ks}(\mathcal{E}) = -1/2n_0^2 - (n_0 - k - s)(\omega \mp \omega_c/2) + E^j(\mathcal{E}), \quad (6)$$

similar to the case with no magnetic field present [10]. The ''ground state'' Trojan wave packet can be now approximated in the rotating frame [10,15] also by a Gaussian product

$$\Psi_+(\mathbf{r},t) = N_+ e^{i(n_0-1)\phi} e^{-(\omega/2)(r-r_0)^2} \times e^{-(\omega/2)r_0^2\theta^2} e^{-\beta(\omega/2)r_0^2(\phi-\omega t)^2}, \quad (7)$$

with the rotating frame energy in the magnetic field

$$E_g(\mathcal{E}) = -1/2n_0^2 - (n_0 - 1)(\omega \mp \omega_c/2) + E^0(\mathcal{E}). \quad (8)$$

For the electromagnetic field with the opposite helicity ($\omega \to -\omega$) the wave packet rotates in the opposite direction and its energy is

$$E_g(\mathcal{E}) = -1/2n_0^2 - (n_0 - 1)(\omega \pm \omega_c/2) + E^0(\mathcal{E}). \quad (9)$$

Therefore in a weak magnetic field the energy of two ''ground-state'' Trojan packets moving in two circularly polarized fields with the same field strengths and opposite helicity differ by the Zeeman splitting

$$\Delta E = (n_0 - 1)\omega_c, \quad (10)$$

proportional to the packet angular momentum.

Note that it is the large angular momentum of the component packet that makes it distinctive and best designed for the observation of the magnetic field influence on the interference. For the packets in the breathing mode like the ones reported in [1] the effect of the magnetic field will be negligible within similar considerations since no angular momentum leading to the Zeeman splitting is carried.

The packet state also exists in a linearly polarized field [16]. In that case a twin pair of states corresponds to two wave packets moving around elliptical, almost circular, orbits with opposite angular momenta. The consequence of the linearity of the Schrödinger equation is that a coherent superposition of those states, with, for example, equal amplitudes, will also be supported by a linearly polarized field [16]. This coherent superposition will therefore strongly interfere twice during one optical cycle, when the well localized components of the state ''collide'' and pass through each other. In this case, however, in contrast to the state observed experimentally in [1], the electron has a fully three dimensional dual nature and exists simultaneously at two places at the same time in all spatial dimensions.

Let us consider the influence of the magnetic field on the probability density $|\Psi_c(\mathbf{r},t)|^2$ calculated from the coherent superposition of state (7) and its counter-rotating twin with equal amplitudes

$$\Psi_c(\mathbf{r},t) = 1/\sqrt{2}\,[\Psi_+(\mathbf{r},t) + \Psi_-(\mathbf{r},t)]. \quad (11)$$

Because two energies of those two components differ by the Zeeman splitting, the phase difference between them after half a cycle is

$$\Delta\phi = \pi(n_0 - 1)\,\omega_c/\omega\,. \quad (12)$$

This phase difference leads to a shift of the interference pattern between two components by $\Delta\phi/2n_0$. Note that since $n_0 \approx n_0 - 1$ for large $n_0$ this can be rewritten as

$$\Delta\phi = \pi n_0^4 \omega_c = \pi r_0^2 \omega_c = \Phi_m = e/\hbar\,\Phi_m\,. \quad (13)$$

The coefficient $\pi r_0^2$ is just the area of the packet orbit and $\Phi_m$ is the magnetic flux cutting the area, so expression (12) coincides with the expression for the Aharonov-Bohm shift [5,6]. Indeed the geometry of the quantum state realizes a standard geometry of the AB experiment since two wave packets move along two paths that draw a closed contour with magnetic flux. It should be pointed out that this AB shift cannot be considered as a result of the AB effect for which no measurable magnetic field should penetrate the wave packet trajectory [6,7,17,18]. Our case represents the alternative consistent with a general result for the AB shift. The phase difference due to the magnetic flux occurs no matter if the component electron beams (component wave packets here) enter the magnetic flux region or not [6].

In order to check these predictions based on a large number of approximations we have solved the time dependent Schrödinger equation in two spatial dimensions using the split operator method [19]. The Hamiltonian is

$$H = \mathbf{p}^2/2 - 1/r + \mathbf{E}(t)\cdot\mathbf{r} + (\omega_c/2)\,L_z + \tfrac{1}{8}\,\omega_c^2(x^2+y^2) \quad (14)$$

with

$$\mathbf{E(t)} = \vec{E}_+(t) + \vec{E}_-(t). \quad (15)$$

First we have generated a coherent superposition of two counterpropagating Trojan wave packets by adiabatic switching of a linearly polarized electromagnetic field without the magnetic field ($\omega_c = 0$) [10]. The field envelope $\mathcal{E}$ was changing from 0 to $\mathcal{E}_0 = 0.016\omega^{-4/3}$ during 20 cycles according to the exponential envelope $\mathcal{E}(t) = \mathcal{E}_0 e^{-0.2(t-20)}$, which was originally used in our numerical experiments for circular polarization [10]. The initial state was an even superposition of two circular states

$$\Psi_c(r,\phi,0) = NR_{n_0,n_0-1}(r)[e^{i(n_0-1)\phi} + e^{-i(n_0-1)\phi}] \quad (16)$$

for $n_0 = 20$, with the Kepler frequency equal to the frequency of the field ($\omega = 1/20^3$) and the opposite angular momentum. Figure 1 shows a typical one-cycle time evolution of the state after the electromagnetic field reached its steady value in zero magnetic field. A strong interference pattern appears on one and the other side of the nucleus twice during a cycle when $t \approx j\pi/\omega$ .

In order to demonstrate the influence of a weak magnetic field on the state evolution we have solved the time dependent Schrödinger equation with the Hamiltonian (14) for different values of the magnetic field $\omega_c$ starting from 0 and ending with $\omega_c = 2\omega/n_0$, which corresponds to a net shift of the interference pattern of the probability density by $2\pi/n_0$ (two fringes) per one optical cycle. The initial state was the two-packet state generated after 20 cycles of adiabatic switching of the linearly polarized field in zero magnetic field. Figures 2 and 3 show the results. Both figures show the probability density calculated from the numerically obtained wave function around the circle with the radius $r = n_0^2$, which

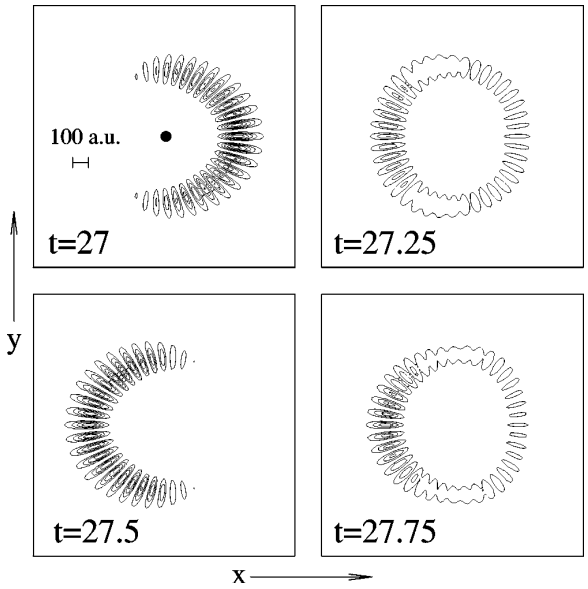


FIG. 1. Typical one-cycle steady field ($\mathcal{E}=0.016\omega^{-4/3}$) evolution of two-packet state ($\mathcal{E}=0.016\omega^{-4/3}$). Strong interference pattern appears twice a period when the two packet components pass through each other. The gauge on the left side of plot at $t=27$ indicates the distance equal to 100 atomic units. The black dot in the center indicates the position of the nucleus ($x=y=0$). The time units are optical cycles.

corresponds to the radial maximum of the wave function (11). Figure 2 shows the dependence on the magnetic field of the interference pattern obtained for the fixed time corresponding to the maximum interference between packet components. Figure 3 shows the $2\pi$ angle phase shift when the magnetic flux that cuts the packet orbit changes by one fluxon ($h/2e$) (note that the packet pair draws a closed contour around the orbit area twice per cycle). The difference between the patterns for different times in Fig. 2 shows that the accumulation of quantum phase is proportional to the number of times the packet pair sweeps the orbit. This time accumulation of phase is shown directly in Fig. 3, which contains the explicit dependence of the interference pattern on time for different magnetic field strengths. One can observe a clear drift of the quantum phase from cycle to cycle. Note that the envelope of the interference signal is not perturbed, which confirms negligible influence of the magnetic field on the component packet trajectories.

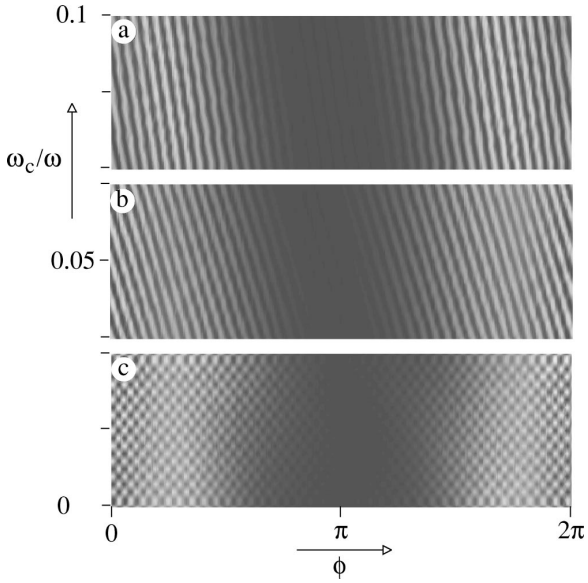


FIG. 2. Dependence of the interference pattern on the strength of the magnetic field at the end of (a) first, (b) second, and (c) fifth optical cycle of a steady field evolution. Gray plots show probability density $|\Phi(\phi,r=n_0^2)|^2$ of the wave function around a circle with radius equal to the radius of the packet orbit. Horizontal axis extends over the full $2\pi$ angle. Magnetic field (vertical axis) changes from 0 to $\omega_c=2\omega/n_0$.

The new experimental technique of generating half-cycle pulses has made it possible both to create atomic wave packets and to probe their momentum distributions [20]. The condition of a successful probing is that the duration of the pulse must be much shorter than the characteristic time related to the wave packet dynamics.

Now we consider ionization of the state (11) by such an ultrashort half-cycle pulse at the time $t$. When the pulse is much shorter than a period of the linearly polarized field it can be represented by an extra potential [21]

$$V_\delta(\mathbf{r},t)=Fx\delta(t), \tag{17}$$

where $F$ is a total impulse given to the electron by the pulse. The quantum state just after its action is

$$\Psi_c(\mathbf{r},t+\epsilon)=e^{-iFx}\Psi_c(\mathbf{r},t). \tag{18}$$

If $\phi_k(\mathbf{r})$ is a continuum state, the differential ionization cross section for $\delta$-pulse ionization is [22]

$$\frac{d\sigma}{d\Omega}=\rho(k)\left|\int \phi_k(\mathbf{r})\Psi_c(\mathbf{r},t+\epsilon)d\mathbf{r}\right|^2, \tag{19}$$

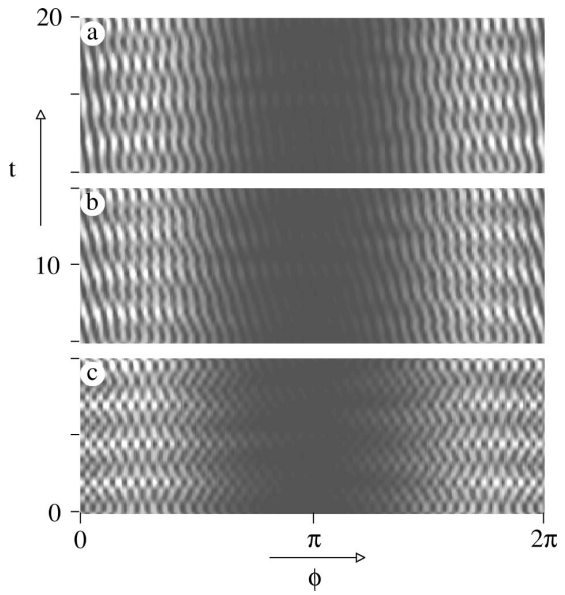


FIG. 3. Time dependence of the interference pattern for different magnetic field strengths (a) $\omega_c=2\omega/n_0^2$, (b) $\omega_c=4\omega/n_0^2$, (c) $\omega_c=10\omega/n_0^2$. Gray plots show probability density $|\Phi(\phi,r=n_0^2)|^2$ of the wave function around the circle with radius equal to the radius of the packet orbit. Each plot shows 20 patterns, each taken at the end of each cycle of 20 cycles of steady field evolution.

where $\rho(k)$ is the density of states around $\phi_k$. After approximating the components of $\Psi_c$ by Gaussians in Cartesian coordinates [9] and the continuum state by a plane wave $\phi_k(\mathbf{r})=e^{i\mathbf{k}\cdot\mathbf{r}}/\sqrt{V}$, this cross section can be calculated analytically and has a maximum amplitude as a function of the magnetic field $\omega_c$ for $t=\pi(1+4j)/2\omega$ and $\mathbf{k}=-\hat{x}(\omega r_0+F)$. This means that the ionization is most magnetic field sensitive when it happens 1/4 of a cycle before and after the state components interfere most in real space, in the direction of the $\delta$ pulse, and for the momentum of the ionized electron, which is a sum of the pulse impulse and the momentum of each of the packet components. In the case of this resonant momentum transfer the cross section can be found as

$$\frac{d\sigma}{d\Omega}=\frac{(\omega r_0+F)^2}{\pi^{3/2}\omega^{3/2}}\frac{\sqrt{\beta}}{(1+\beta)}\cos^2[\Phi_m(1/4+j)]. \qquad (20)$$

In this case the oscillations occur but with a period that is an integer fraction of a single fluxon $h/2e$ depending on the number $j$ of cycles before the probing pulse is launched (fractional AB oscillations). Figure 4 shows the differential cross section (19) as a function of time and the magnetic field calculated from the numerical solution for the optimal ionization. For a fixed delay time this quantity oscillates as a function of the magnetic field strength with the highest amplitude when $t\approx(1+4j)\pi/2\omega$ as predicted. As the number of cycles $j$ grows, the number of oscillations also grows, which shows that the ionization becomes more and more sensitive to the magnetic field. For example, for an atom with $n_0\approx 60$ the change of a magnetic field by $10^{-5}$ T changes the oscillatory factor in the expression (20) from 0 to 1 if the ionizing $\delta$ pulse was launched after 1000 cycles.

In conclusion, we have constructed and observed numerically, a quantum state for which the observation of

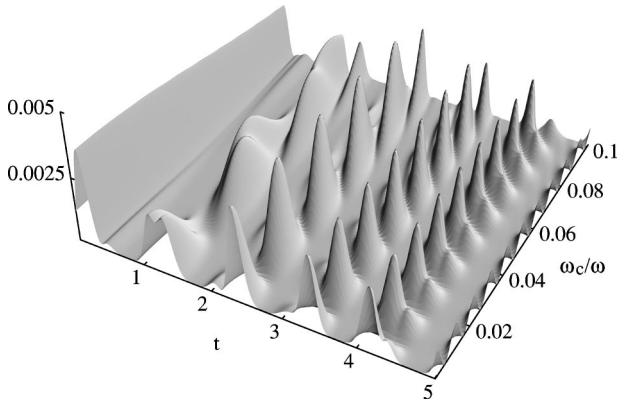


FIG. 4. Differential cross section for $\delta$-pulse ionization (19) for resonant and parallel momentum transfer $\mathbf{k}=-\hat{x}(\omega r_0+F)$ (up to the multiplicative $F$-dependent factor from the density of states). The numerical solution of the Schrödinger equation with Hamiltonian (14) is used, and a plane wave as continuum state. The time units are optical cycles.

Aharonov-Bohm oscillations in a single atom is possible in an experiment analogous to the one reported in [1] using the half-cycle pulse probing technique. Those oscillations originate from Zeeman splitting between the energies of counterrotating components and the peculiar time dependence of this state. Of course the success of such an experiment will depend on generating Trojan packets, which still remains a challenge for experimental physics.

I would like to thank I. Bialynicki-Birula, J. H. Eberly, C. R. Stroud, Jr. as well as C. K. Law and J. West for stimulating comments and suggestions. Research reported here was supported by the Rochester Theory Center for Optical Science and Engineering and by the National Science Foundation under Grant Nos. INT93-11766, PHY94-08733, and PHY94-15583.

[1] M. W. Noel and C. R. Stroud, Jr., Phys. Rev. Lett. **75**, 1252 (1995).
[2] L. S. Brown, Am. J. Phys. **41**, 525 (1973).
[3] J. A. Yeazell and C. R. Stroud, Jr., Phys. Rev. Lett. **60**, 1494 (1988); I. Sh. Averbukh and N. F. Perelman, Acta Phys. Pol. A **78**, 33 (1990); J. A. Yeazell *et al.*, Phys. Rev. A **40**, 5040 (1989); J. A. Yeazell *et al.*, Phys. Rev. Lett. **64**, 2007 (1990).
[4] For review of electron interference experiments see G. F. Missiroli, G. Pozzi, and U. Valdre, J. Phys. E **14**, 649 (1981).
[5] Y. Aharonov and D. Bohm, Phys. Rev. **115**, 485 (1959).
[6] M. Peshkin and A. Tonomura, *The Aharonov-Bohm Effect* (Springer-Verlag, Berlin, 1989).
[7] For discussion of experimental conditions for the AB shift in accessible and inaccessible fields see A. Tonomura, Physica B **151**, 206 (1988).
[8] See for example K. N. Pichugin and A. F. Sadreev, Zh. Exp. Theor. Fiz. **109**, 546 (1996) [JETP **82**, 290 (1996)], and references therein.
[9] I. Bialynicki-Birula *et al.*, Phys. Rev. Lett. **73**, 1777 (1994); M. Kalinski *et al.*, Phys. Rev. Lett. **52**, 2460 (1995).
[10] M. Kalinski and J. H. Eberly, Phys. Rev. A **53**, 1715 (1996).
[11] D. Delande *et al.*, Europhys. Lett. **32**, 107 (1995); J. Zakrzewski *et al.*, Phys. Rev. Lett. **75**, 4015 (1995).
[12] H. Klar, Z. Phys. D **11**, 45 (1989); D. Farrely and T. Uzer, Phys. Rev. Lett. **74**, 1720 (1995).
[13] D. Farrelly *et al.*, Phys. Lett. A **204**, 359 (1995); E. Lee *et al.*, Phys. Rev. Lett. **75**, 3641 (1995); A. F. Brunello *et al.*, *ibid.* **76**, 2874 (1996).
[14] M. Kalinski and J. H. Eberly, Phys. Rev. Lett. **77**, 2420 (1996).
[15] We neglect here the influence of the linear term in the pendular Hamiltonian (5) on the parameters of the wave function.
[16] M. Kalinski and J. H. Eberly, Phys. Rev. A **52**, 4285 (1995).
[17] S. M. Roy, Phys. Rev. Lett. **44**, 111 (1980).
[18] A. Tonomura, Jpn. J. Appl. Phys., Part 1 **34**, 2951 (1995).
[19] R. Grobe and J. H. Eberly, Phys. Rev. A **47**, R1605 (1993).
[20] R. R. Jones, Phys. Rev. Lett. **76**, 3927 (1996).
[21] V. Enss, Phys. Rev. A **50**, 1578 (1994).
[22] D. Belkić, J. Phys. B **14**, 1907 (1981).